

Hadronic Energy Calibration of the H1 Experiment

Jörg Marks

University of Heidelberg

for the



H1 Collaboration

Outline

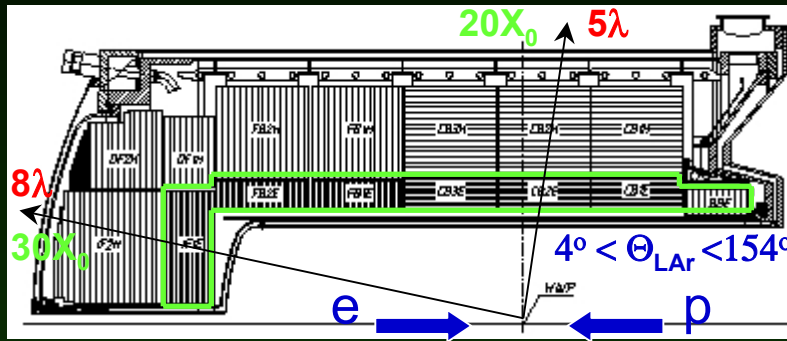
- ✓ H1 LAr calorimeter
- ✓ Hadronic energy reconstruction
- ✓ Results of CERN test beam measurements
- ✓ LAr Purity monitoring
- ✓ HV curves with μ 's
- ✓ Hadron calibration in ep data
- ✓ New energy weighting method
- ✓ Summary



The H1 LAr Calorimeter

➤ 8 self supporting wheels

➤ 8 fold structure for each wheel



Hadronic part

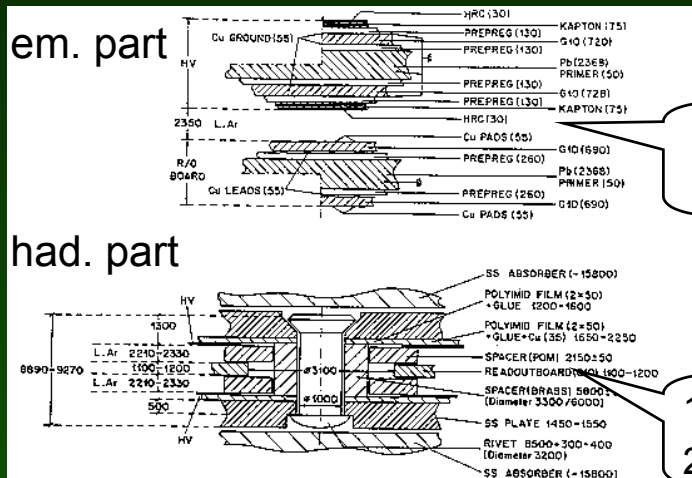
Granularity: 50 - 2000 cm²

Long. Segmentation: 4-6

Number of chan. : 13568

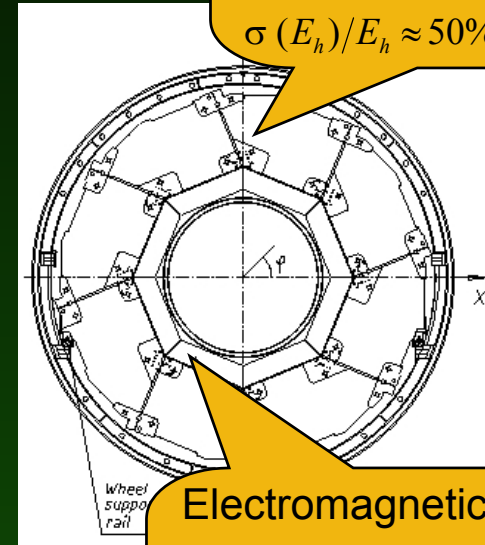
$\sigma(E_h)/E_h \approx 50\%/\sqrt{E_h} \oplus 2\%$

➤ Readout cell structure



2.40 mm Pb
2.35 mm LAr

19 mm steel
2.4 mm LAr



Electromagnetic part

Granularity: 10 - 100 cm²

Long. Segmentation: 3-4

Number of chan. : 30784

$\sigma(E_e)/E_e \approx 11\%/\sqrt{E_e} \oplus 1\%$



Electronic Calibration and Noise

➤ Electronic Calibration

- ❖ Two calibration systems: cold and warm (as backup solution)
- ❖ Stability within 10^{-3}
- ❖ Online charge conversion in the front end DSPs using calibration data from 3rd order polynomial fits

➤ Noise

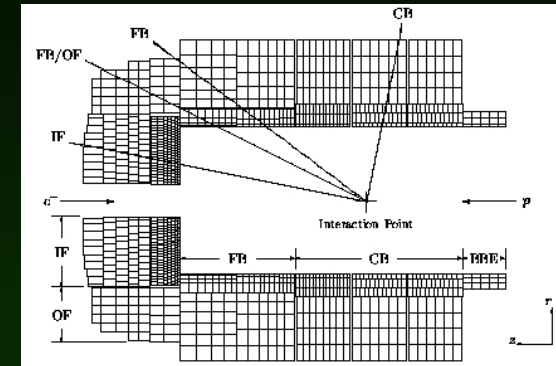
- ❖ Special noise suppression including negative noise contributions
- ❖ $1 \sigma_{\text{noise}}$ values:

	Central Barrel	Inner Forward
<i>Electromagnetic part</i>	<i>30 MeV / 0.25 mips</i>	<i>15 MeV / 0.15 mips</i>
<i>Hadronic part</i>	<i>30 MeV / 0.15 mips</i>	<i>24 MeV / 0.15 mips</i>
- ❖ Topological noise suppression
- ❖ H1 MC simulations include measured noise from random triggers

CERN Test Beam Measurements

➤ Extensive test program at CERN SPS with e, π and μ beams

- ❖ Measurements with calorimeter prototypes as proof of principle
- ❖ Calibration runs with stacks of each final H1 module
- ❖ Tests of z and ϕ crack regions



➤ Determine calibration constants of the electromagnetic scale

Data: Q_i $\xrightarrow{(c_{EMC}^{exp}, c_{HAC}^{exp})_{wheel}}$ E_i^0 and MC: E_i^{vis} $\xrightarrow{(c_{EMC}^{MC}, c_{HAC}^{MC})_{wheel}}$ E_i^0

such that
$$E_{rec}^{exp} = c_{EMC}^{exp} \sum_i^{EMC} Q_i = E_{rec}^{MC} = c_{EMC}^{MC} \sum_j^{EMC} E_j^{vis}$$



$$c_{EMC}^{exp} = 3.55 GeV / pC$$

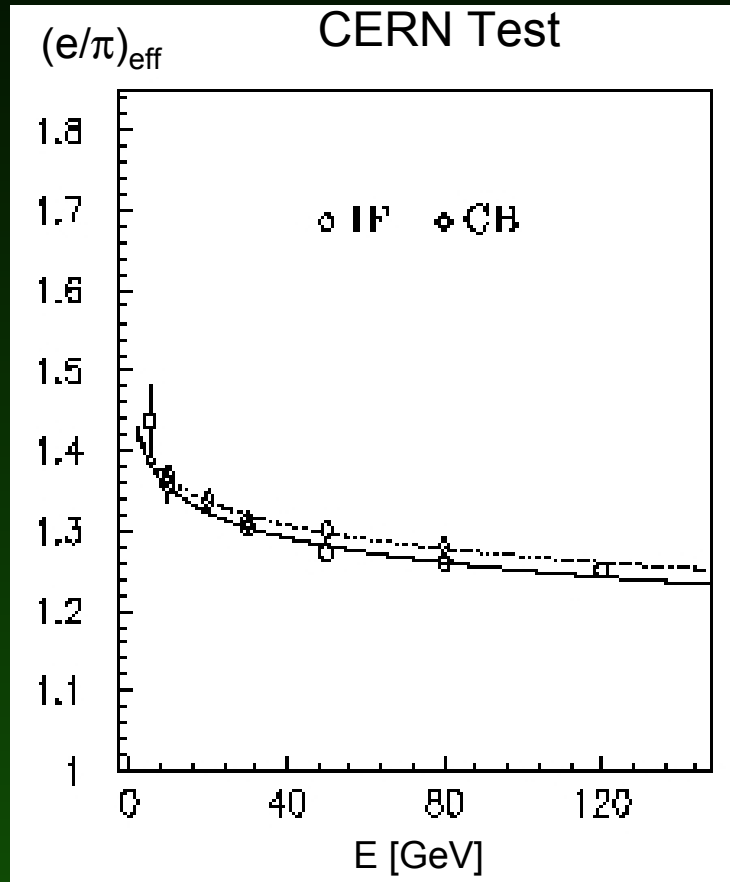
$$c_{HAC}^{exp} = 7.10 GeV / pC$$

$$\Delta c_{EMC}^{exp} / c_{EMC}^{exp} = 3\%$$

$$\Delta c_{HAC}^{exp} / c_{HAC}^{exp} = 4\%$$

Energy Measurement of π 's

➤ Measurement of the e/π ratio



- ❖ $e/\pi > 1 \Rightarrow$ non compensating Calorimeter
- ❖ $f_{\text{em}} \sim \log E_{\text{beam}} \Rightarrow$ non linear response
- ❖ π^0 fluctuations cause non gaussian contribution to the energy resolution
- **Energy weighting**
 - \Rightarrow equalize the response of the electromagnetic and hadronic component in the shower
- ❖ software method which requires fine granularity of the calorimeter

Energy Weighting in H1 (1)

- Identify the primary electromagnetic component ($E_{\text{cluster}} > 1 \text{ GeV}$)
 - ❖ Energy in the EMC
 - ❖ Fraction of energy in the first layer
 - ❖ Fraction of energy in the 4 most energetic cells
- Energy weighting of hadronic objects
 - ❖ Hadronic cluster are prominent cluster ($\sum (E_i/\sigma_{\text{noise}})^2)^{1/2} > 8$) penetrating deeply into the calorimeter
 - ❖ Hadronic objects are formed by hadronic cluster together with cells in a cylinder of $r_{\text{EMC}} < 25 \text{ cm}$ and $r_{\text{HAC}} < 50 \text{ cm}$ in the direction of the I.P.
 - ❖ Apply the weighting function to the cells of the hadronic objects

$$E_F = \omega \cdot E_I^i$$

with

$$\omega = C_1 \cdot e^{-C_2 \cdot \frac{E_i^{em}}{Vol_i}} + C_3$$

for $E_{\text{group}} > 10 \text{ GeV}$

Energy Weighting in H1 (2)

➤ Weighting parameters

$$C_{1/2} = C_{1/2}(E_{group})$$

$$C_3 = C_3(E_{group}, \theta)$$

- generated using jet data of detailed MC simulations
- different for EMC and HAC
- parametrization of the jet energy E_{group} (determined in 10° cones) and of θ

➤ Hadronic energy reconstruction at low energies

- ❖ Linear correction for $E_{group} < 7$ GeV
using the measured e/π ratio:

$$E_F = \omega \cdot E_I^i$$

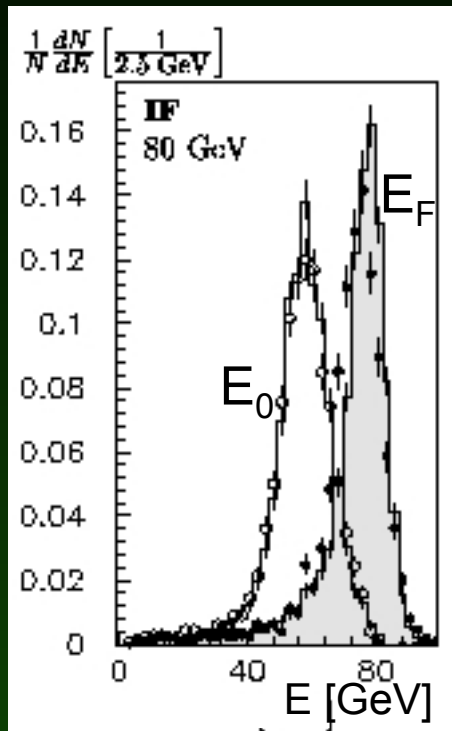
$$\omega^{HAC} = 1.608$$

$$\omega^{EMC} = 1.353$$

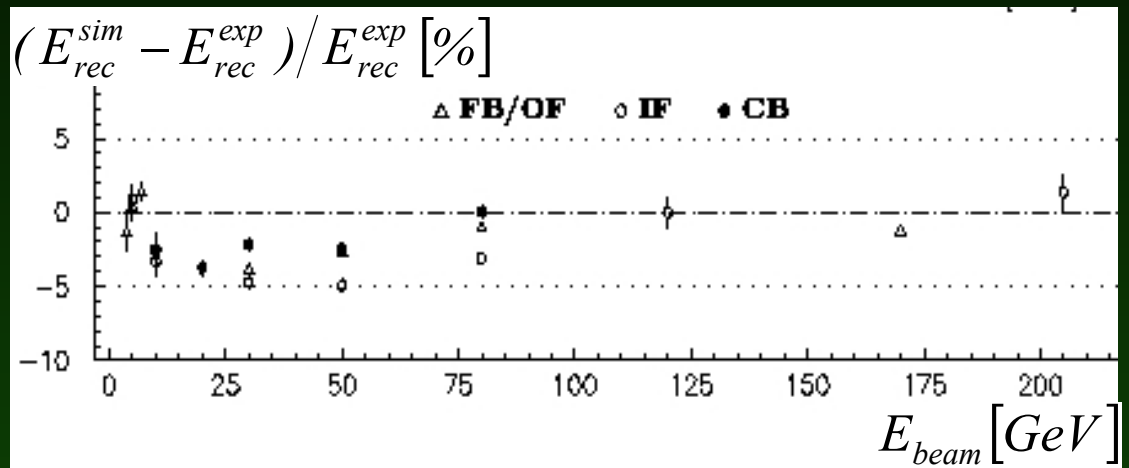
- ❖ Smooth transition between both methods for
 $7 \text{ GeV} < E_{group} < 10 \text{ GeV}$

CERN Test Beam - π Results

➤ Energy measurement of π 's



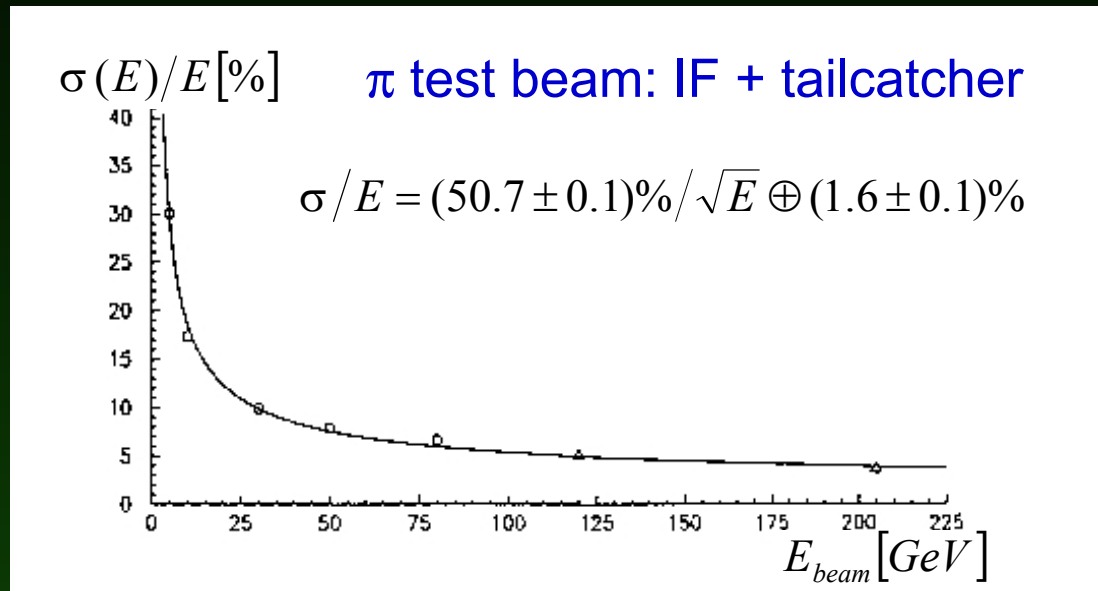
Deviation of the MC simulation from data (final energy scale)



Reconstructed energy
on the E_0 and E_F scale

CERN Test Beam - π Results

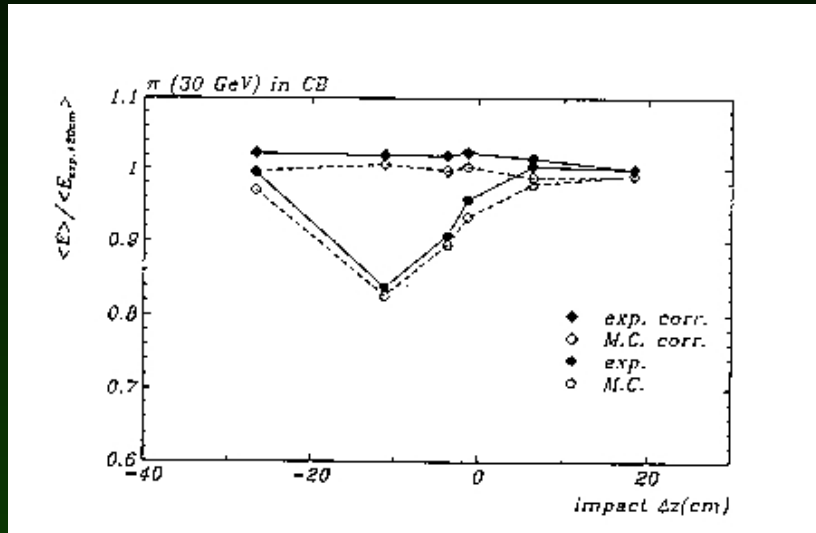
- Energy resolution after energy weighting, Inner Forward calorimeter



- Energy weighting compared to a linear calibration (jets, detailed MC)
 - ❖ Constant term is reduced by factor 2
 - ❖ Sampling term improves by $\sim 30\%$

CERN Test Beam – z, ϕ Cracks

➤ CB2/CB3 z crack in a 30 GeV π beam



❖ z crack is almost pointing to the interaction vertex

❖ Crack correction

$$E_{loss}^j = \beta \cdot f_{loss}^j \cdot \frac{E_r^j \cdot E_l^j}{E_r^j + E_l^j}$$

$$\beta_{em} \neq \beta_{had}$$

❖ Position independent response after the crack correction

❖ Response is well described by the simulation

➤ Crack correction parameters determined for hadrons are used for both shower components

LAr Purity Monitoring System

Aim: control longterm stability of the LAr signal

- Purity measurements by 10 LAr ionization chambers (^{207}Bi and ^{241}Am sources) inside the cryostat

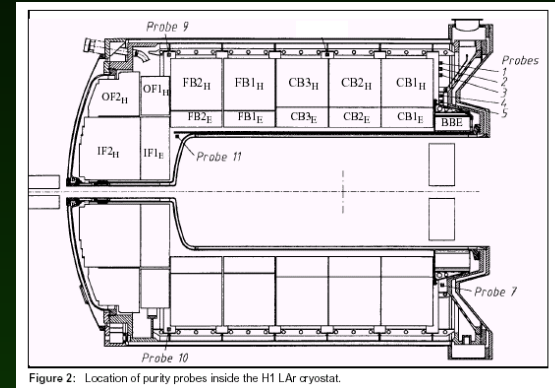
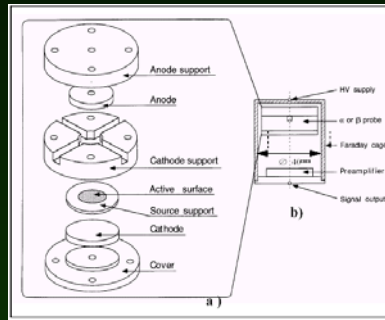


Figure 2: Location of purity probes inside the H1 LAr cryostat.

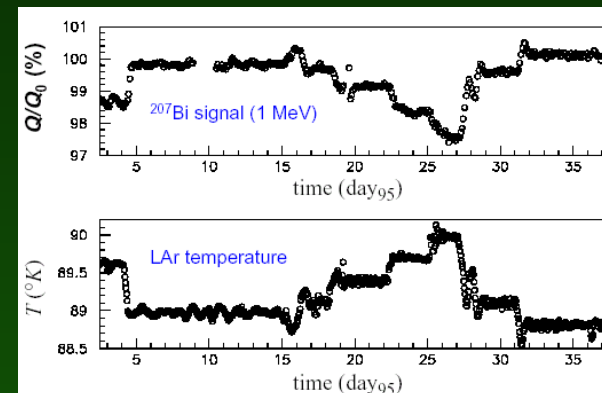
Determine the ionization charge Q and relate the mean free path λ_e

- LAr temperature effect for ^{207}Bi

$$\Delta Q/Q = -\kappa \Delta T, \quad \kappa \cong 1.5 \% / K^{\circ}$$

LAr temperature oscillation

in 24 h operation: $\begin{matrix} +0.1 \\ -0.2 \end{matrix} K^{\circ}$

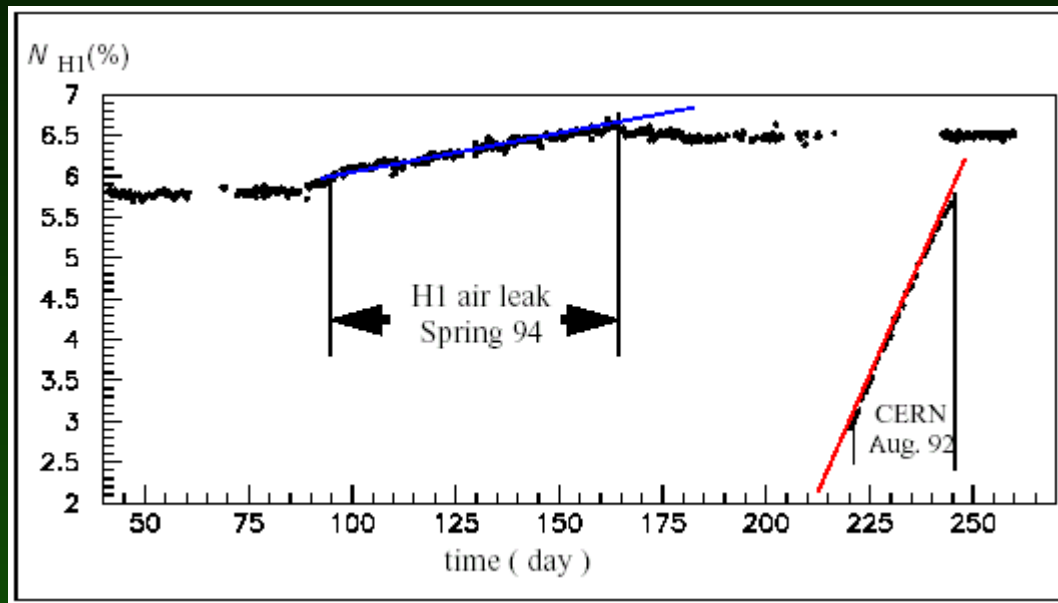


LAr Impurity Measurement (1)

- Impurity N_{H1} of a ^{207}Bi probe converted from the measured charge

During the CERN tests there was a continuous release of impurities into the LAr at the % level / month (no oxygen pollution)

This was a factor 100 larger than the observed measurements in H1

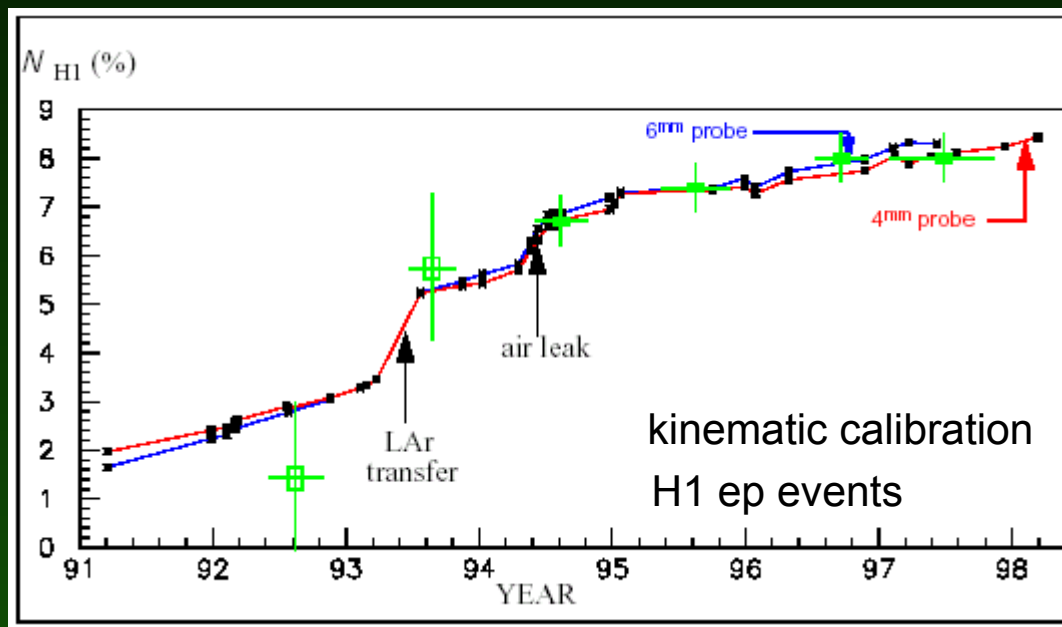


LAr Impurity Measurement (2)

➤ Average impurities N_{H1} in H1 from 91 to 98 using HV curves

Convert HV curves into impurity curves using a relation between the mean free path and the electrical field determined from the data

Obtain the average impurity for fields $0.35 \text{ cm/kV} < E^{-1} < 0.9 \text{ cm/kV}$

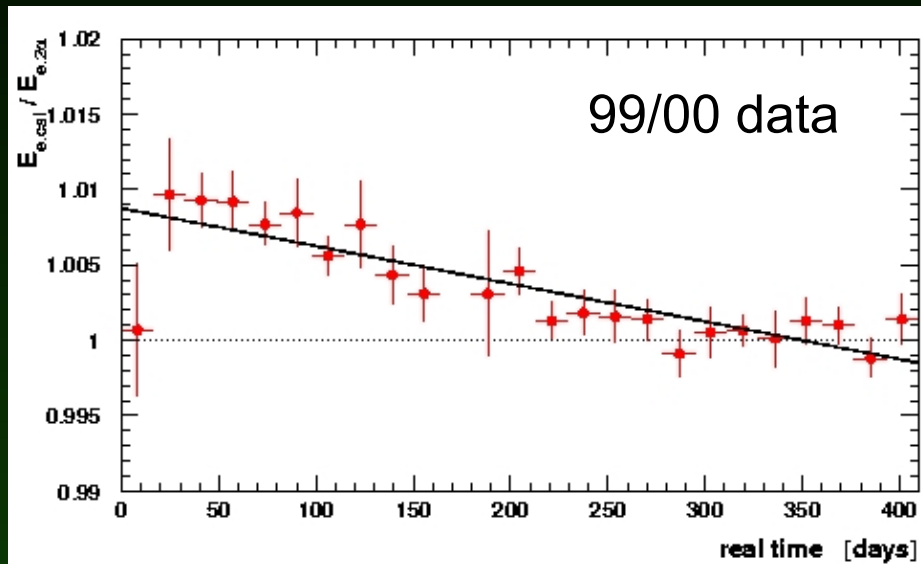


Over 6 years of operation the cumulative effect of the LAr pollution on the energy measurement is $\sim 2.5\%$

Details:
see [hep-ex 0111066](https://arxiv.org/abs/hep-ex/0111066)

LAr Purity Monitoring in ep Data

- Signal degradation directly observed in NC DIS high Q^2 data



Measure $E_{2\alpha}/E_e$ vs time

The sensitivity is clearly on the ‰ level

Use data for the correction

For physics analysis corrections are needed when combining data from different running periods

Still unknown is the sensitivity of the data to temperature gradients
T gradients are stable \Rightarrow covered within the octant wise offline calibration

Charge Collection Efficiency

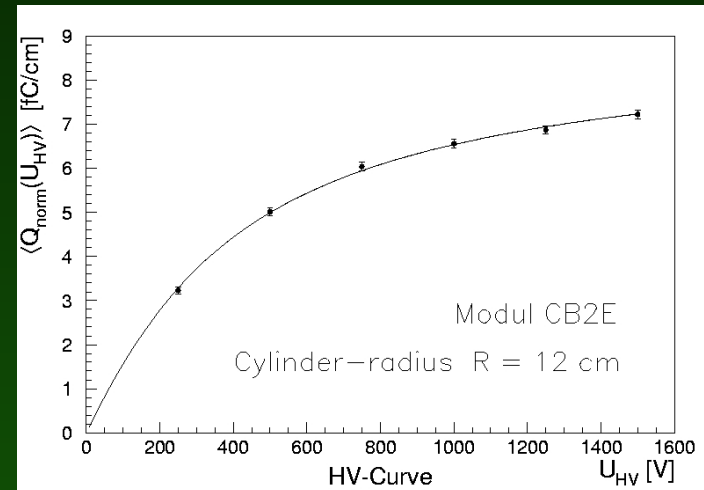
- Measurement of high voltage curves with cosmic and beam halo μ 's
 - ❖ Determine the charge collection efficiency by a fit to

$$\varepsilon(U_{HV}) = \frac{Q(U_{HV})}{Q_0} = 2 \frac{\alpha U_{HV}}{pd^2_{gap}} \left[1 - \frac{\alpha U_{HV}}{pd^2_{gap}} \left(1 - e^{-\frac{pd^2_{gap}}{\alpha U_{HV}}} \right) \right]$$

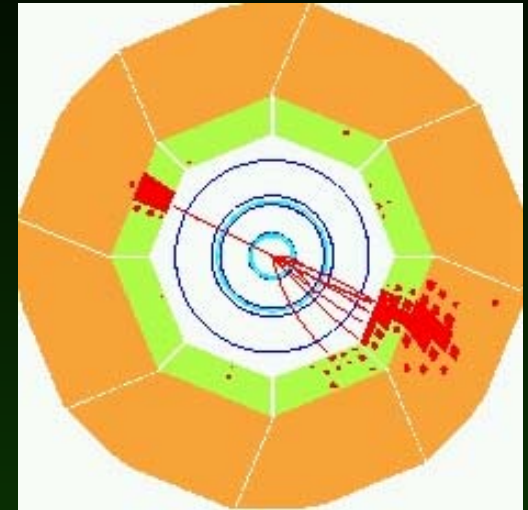
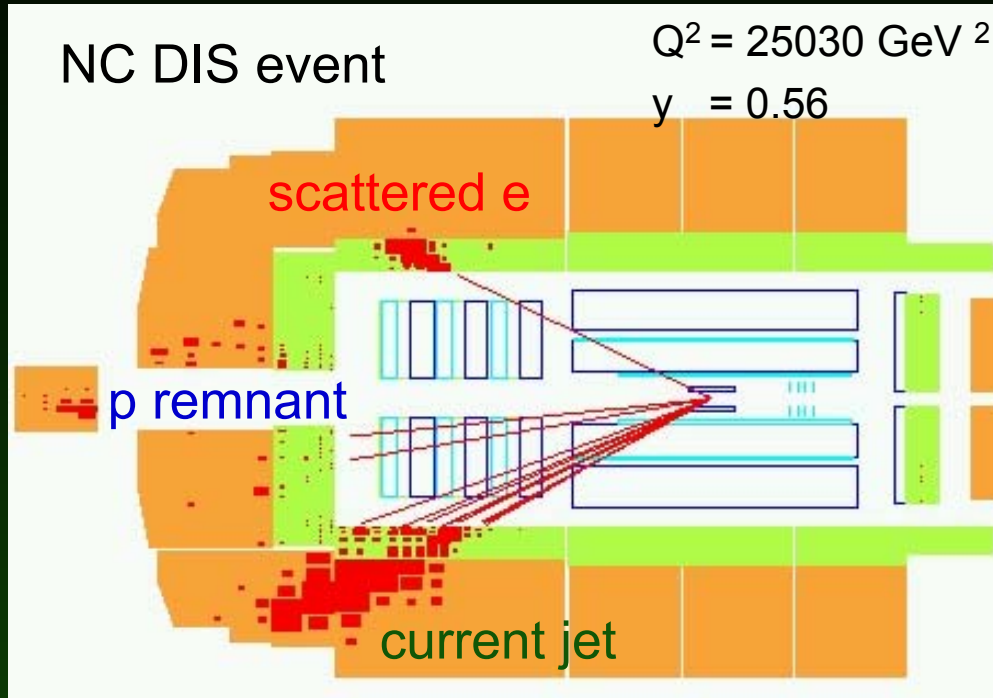
Before the beam operation of H1 in 91/92:
(at $E = 1500$ kV)

$$\varepsilon = 0.944 \pm 0.014$$
$$p = 0.55 \pm 0.14 \text{ ppm}$$

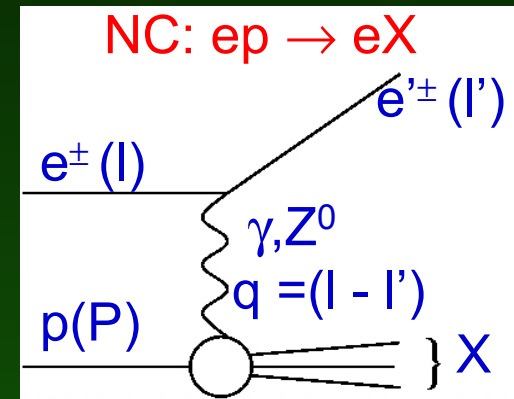
- ❖ Derive wheel wise calibration coefficients in EMC and HAC using cosmic and beam halo μ 's
Difficult: low signal/noise
- ❖ Long term stability checks inside modules



Calibration with NC DIS Data

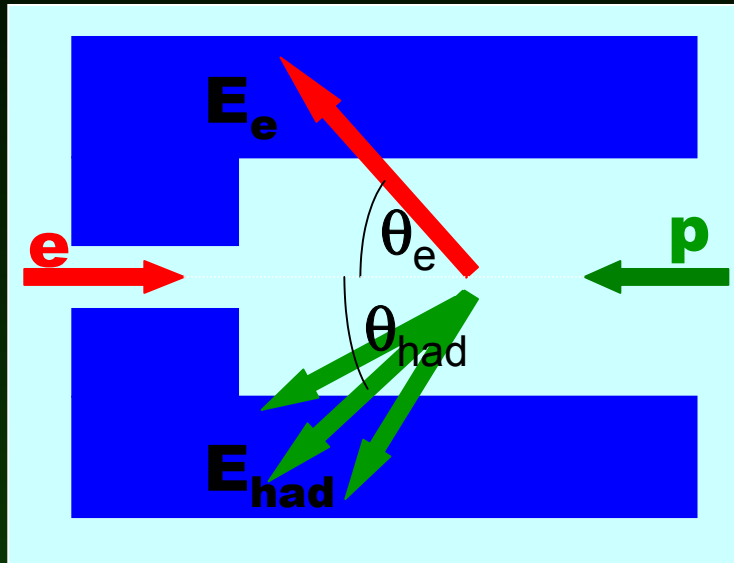


$Q^2 = -q^2$ resolving power of the probe
 $y = (P \cdot q) / (P \cdot l')$ inelasticity parameter
 $x = -q^2 / 2(P \cdot q)$ fraction of p momentum



Measurements and Constraints

➤ Four measurements:



❖ Energy and angle of the scattered lepton and the hadronic final state

❖ Inclusive hadronic angle

$$\tan \frac{\theta_{had}}{2} = \frac{(E - p_z)^{had}}{p_t^{had}}$$

❖ 2 variables describe kinematics

➤ Over constraint system offers calibration and checking possibilities

❖ Transverse momentum (P_t) balance: $P_t^e = P_t^{had}$

❖ Longitudinal momentum ($E-p_z$) balance: $(E-p_z)^e + (E-p_z)^{had} = 2E^e_{beam}$

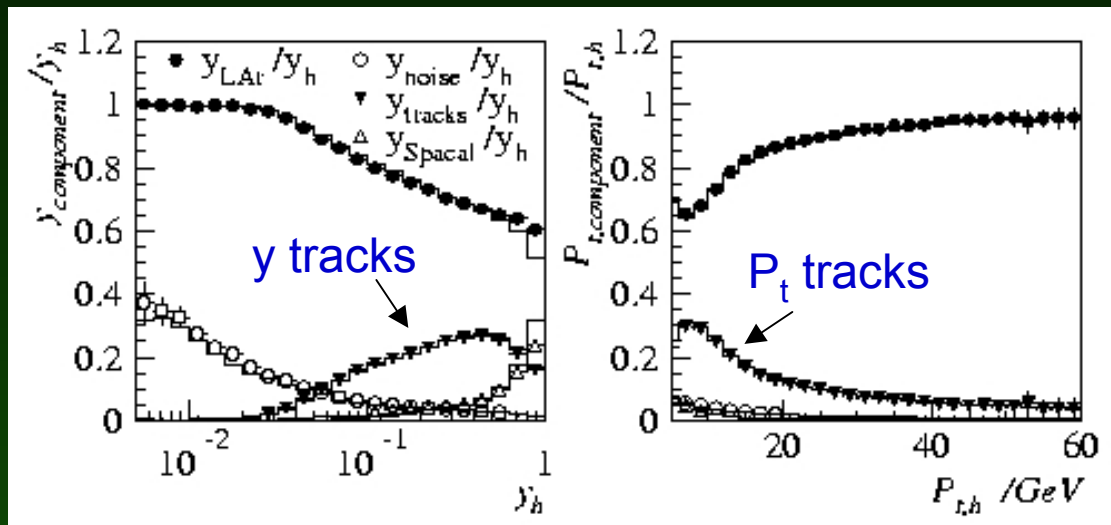
❖ Double angle method: predict E^e, E^{had} from measured (θ_e, θ_{had})

Cluster Track Combination

The hadronic final state is measured using calorimeter energy depositions and low momentum tracks to improve the response.

➤ Cluster track combination

Extrapolate tracks ($p < 2$ GeV) in the central area to the calorimeter and replace E_{cluster} within a radius ($r_{\text{em}} = 25\text{cm}$, $r_{\text{had}} = 50\text{cm}$) by p_{track}

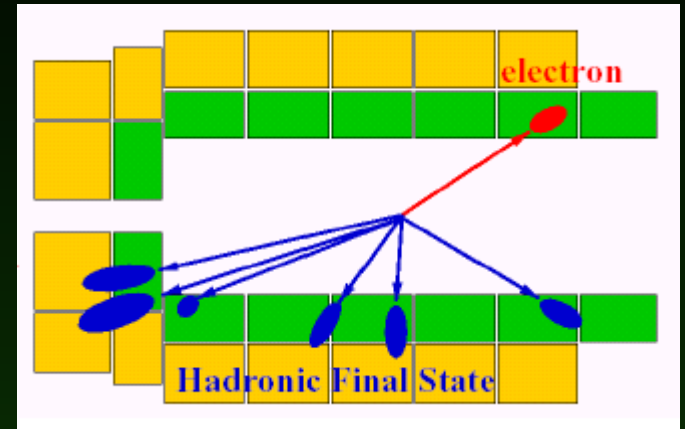
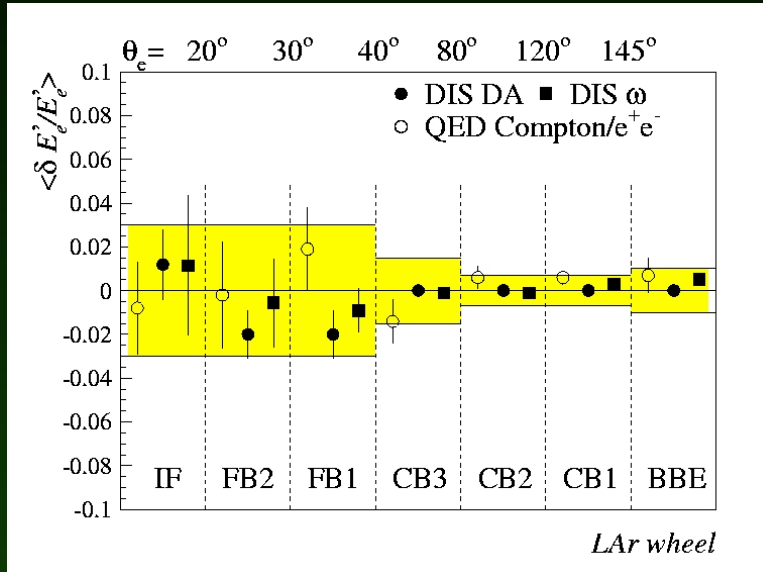


$$y_{\text{had}} = \frac{\sum (E^i - p_z^i)}{2E_{\text{beam}}}$$

Isolated low energy calorimetric deposits are classified as noise

Calibration Fundamentals

- Calibrate the electron using the NC double angle e energy prediction



transverse + longitudinal
momentum balance

Statistical techniques on large samples to establish energy and position dependent hadron calibration

Hadronic Energy Calibration (1)

➤ Calorimeter calibration approach

Determine calibration coefficients for different hardware regions of the LAr calorimeter in order to describe data / MC of various observables (p_t , $E-p_z$, y , Q^2 , ...) in different kinematic regimes

❖ Lagrange Method

$$L = \sum_{i=1}^{events} \frac{1}{\sigma_i^2} \left(p_t^e - p_t^{track} - \sum_{j=1}^M p_{ti}^j \cdot \alpha_j \right)^2 \rightarrow min$$

120 coefficients
(wheel, octant)

❖ Iterative Method

$$\Delta_j = 1 - \sum_{i=1}^{events} \delta^i W_j^i$$

$p_{\perp}^{LAr} =: p_t$ projected onto the electron direction

$$p_{\perp}^{LAr} = \sum_i p_t^i \cdot \cos(\phi^i - \phi^{el})$$

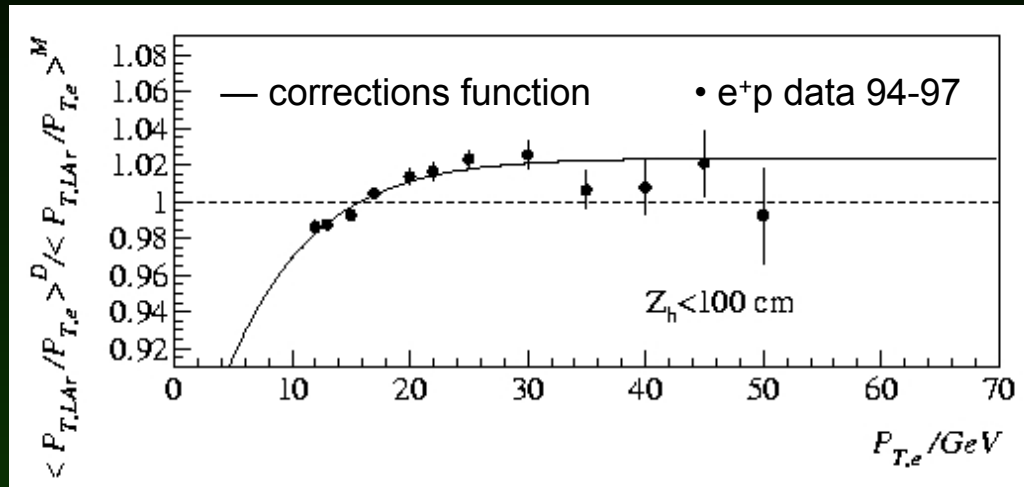
$w_{ev}^j = p_t^j / p_t$ fractional p_t in wheel j

$\delta^{ev} = p_{\perp}^{LAr} / p_t$ event pull

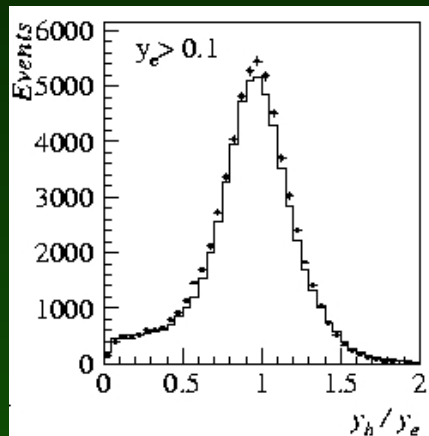
$$\langle \Delta_j^{data} \rangle / \langle \Delta_j^{MC} \rangle \rightarrow 15 \text{ coefficients (wheel wise)}$$

Hadronic Energy Calibration (2)

- p_t dependence of the description of the data by the MC



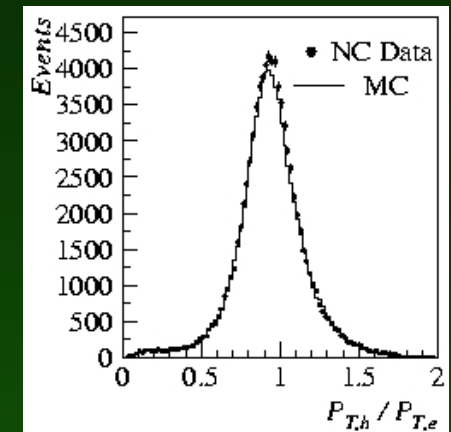
After the correction of the p_t dependence the hadronic energy measurement for data and MC agrees within 2 %



E- p_z measurement

p_t measurement

Final Calibration

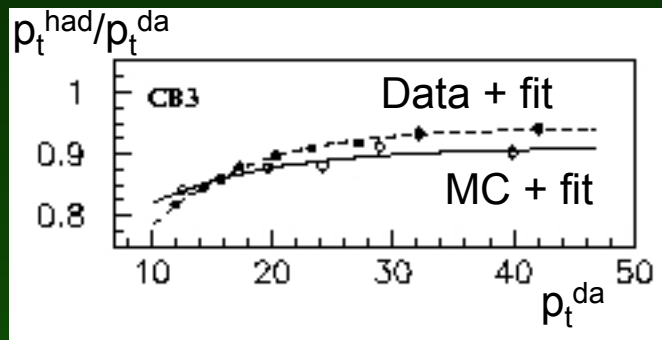


Hadronic Energy Calibration (3)

➤ Alternative approach

(p_t, θ) dependent calibration using the jets of the hadronic final state

- ❖ Select NC DIS high Q^2 (1+1) jet events
- ❖ Adjust $\langle p_t^{\text{had}} / p_t^{\text{da}} \rangle_{\text{data}}$ and $\langle p_t^{\text{had}} / p_t^{\text{da}} \rangle_{\text{MC}}$ in θ_{jet} ranges
- ❖ Fit $p_t^{\text{balance}} = F(\theta_{\text{jet}}, p_t^{\text{da}})$ for data and MC
- ❖ Correct the quantities of each jet iterating with $F(\theta_{\text{jet}}, p_t^{\text{da}})$
- ❖ The method provides an absolute hadronic scale

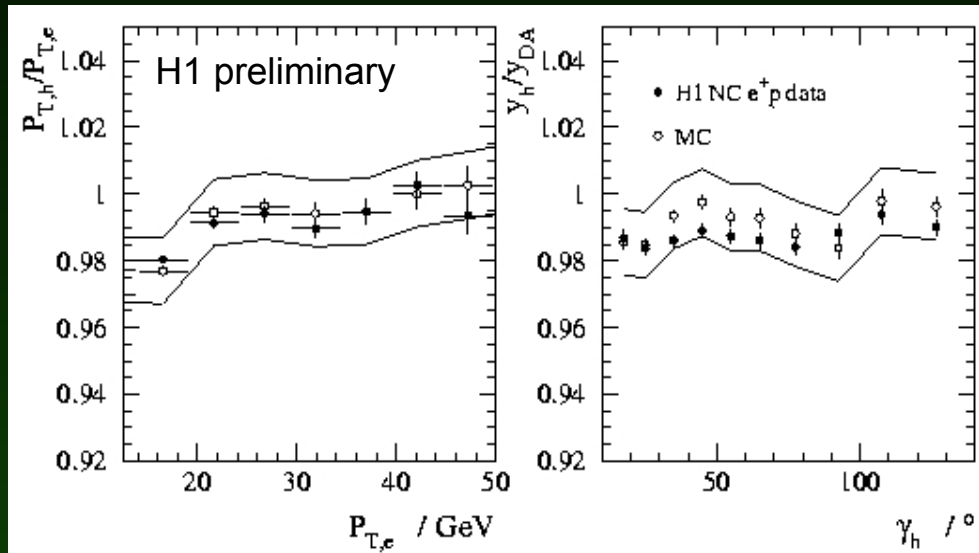


The procedure yields equivalent precision

Hadronic Energy Calibration (4)

- Improved precision of the hadronic scale including all e^+p NC DIS data

$$12 \text{ GeV} < p_t^{\text{had}} < 50 \text{ GeV} \quad \text{and} \quad \gamma_{\text{had}} > 15^\circ$$

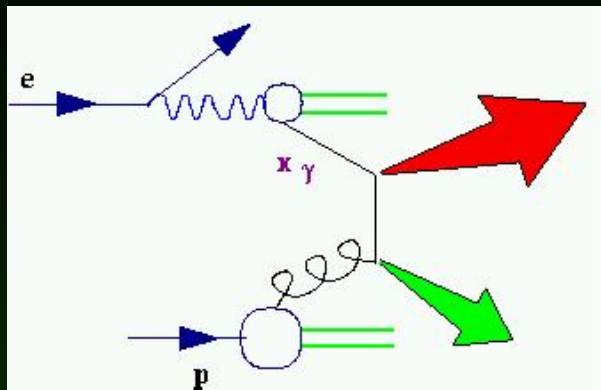


- ❖ Correct the p_t dependence for data and MC in bins of γ_{had}
- ❖ E- p_z and p_t measurement well described within $\pm 1\%$
- ❖ 1% correlated error from electron measurement

- ❖ Wheel dependent calibration from y balance
Adjust y^{had} / y^e for data and MC in different areas of the LAr calorimeter

→ equivalent results

Dijets in Photoproduction



➤ Jet definition

Inclusive k_{\perp} algorithm using energy deposits in the calorimeters and low momentum tracks

➤ Application of the NC DIS high Q^2 calibration

As a cross check: select a NC DIS sample with $E_t^e > 15 \text{ GeV}$ and show that p_t^{had} / p_t^e of the data is described within $\pm 2\%$ by MC

➤ Energy scale error in the dijet data

Deviations for subselections and various dependencies $< 2\%$

➤ Dijet cross section measurement

Hadronic energy calibration is an important aspect

➤ Large transverse energy selection

$$E_t (1. \text{ Jet}) > 25 \text{ GeV}$$

$$E_t (2. \text{ Jet}) > 15 \text{ GeV}$$

Dijet Data – Energy Calibration (1)

➤ Jet Jet balance

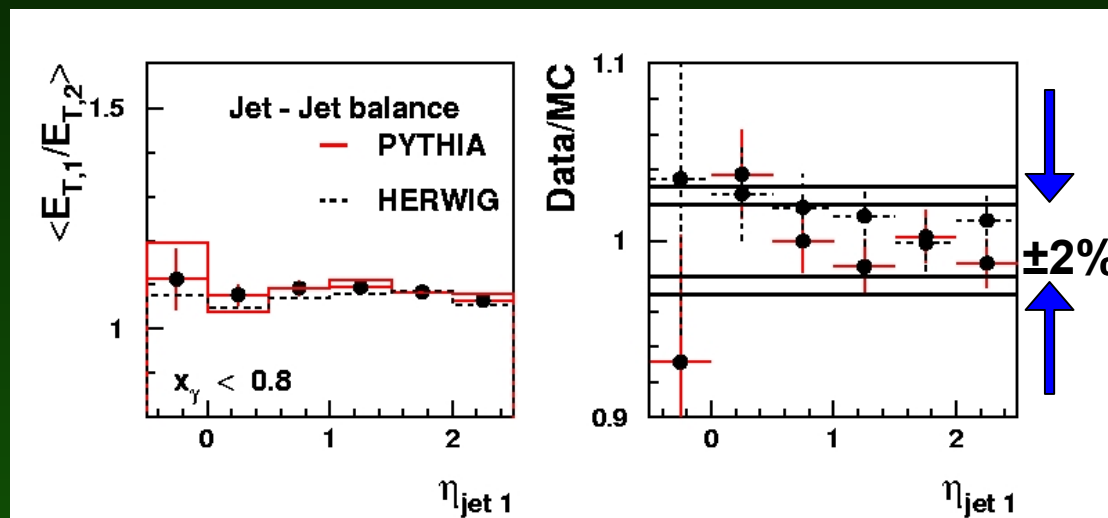
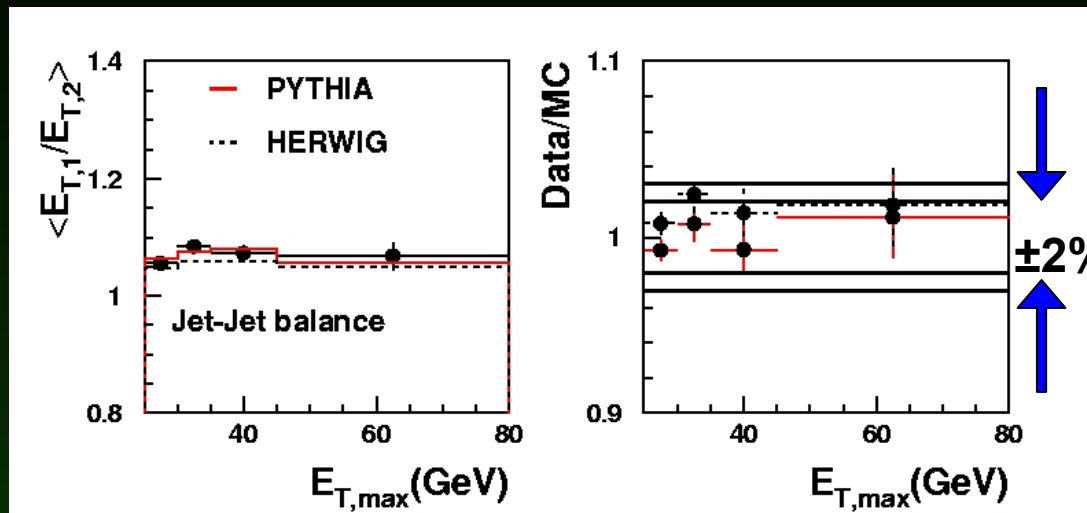
$$E_{t,Jet1} / E_{t,Jet2}$$

❖ $E_{t,Max}$ dependence

❖ η_{Jet1} dependence

❖ $x_\gamma > 0.8$ (direct processes)

❖ $x_\gamma < 0.8$ (resolved processes)



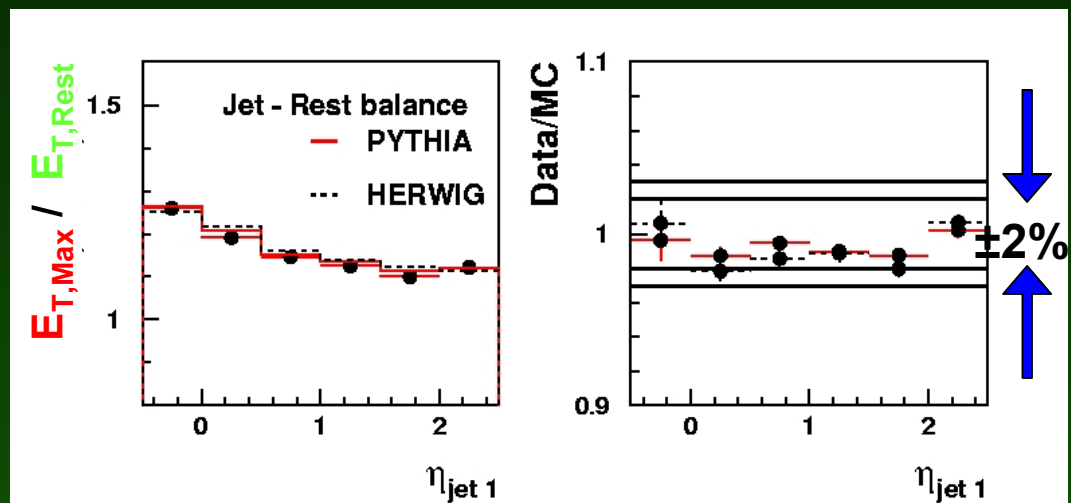
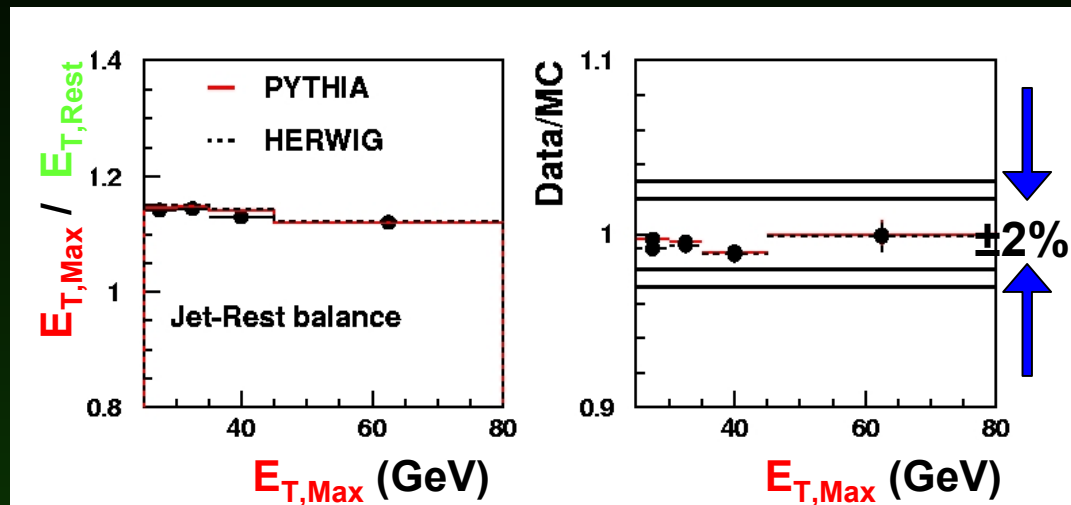
Dijet Data – Energy Calibration (2)

➤ Jet-Rest balance

$$E_{t,Max} / E_{t,Rest}$$

❖ $E_{t,Max}$ dependence

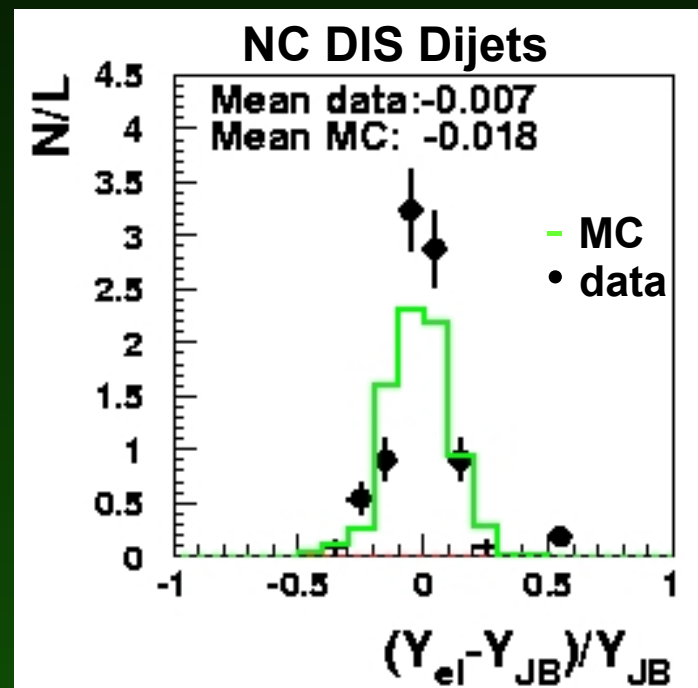
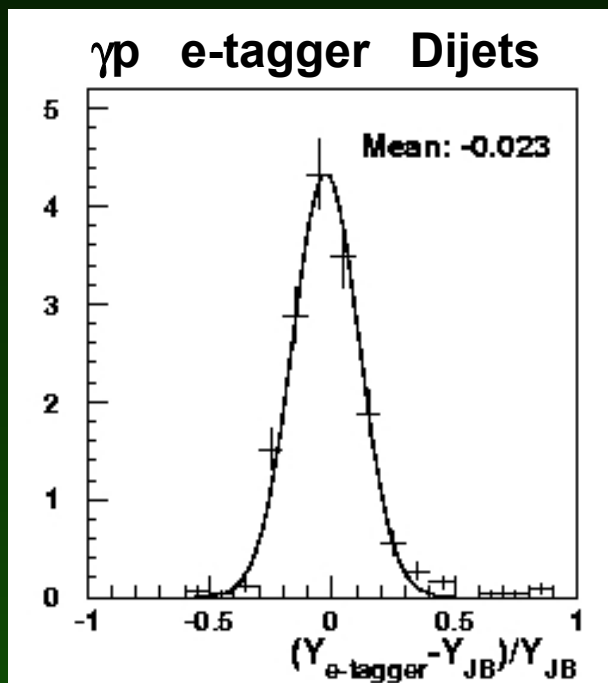
❖ $\eta_{Jet 1}$ dependence



Dijet Data – Energy Calibration (3)

➤ y balance

Compare y_{el} measured with the electron and y_{JB} reconstructed from the hadronic final state



Dijet Data – Calibration Results

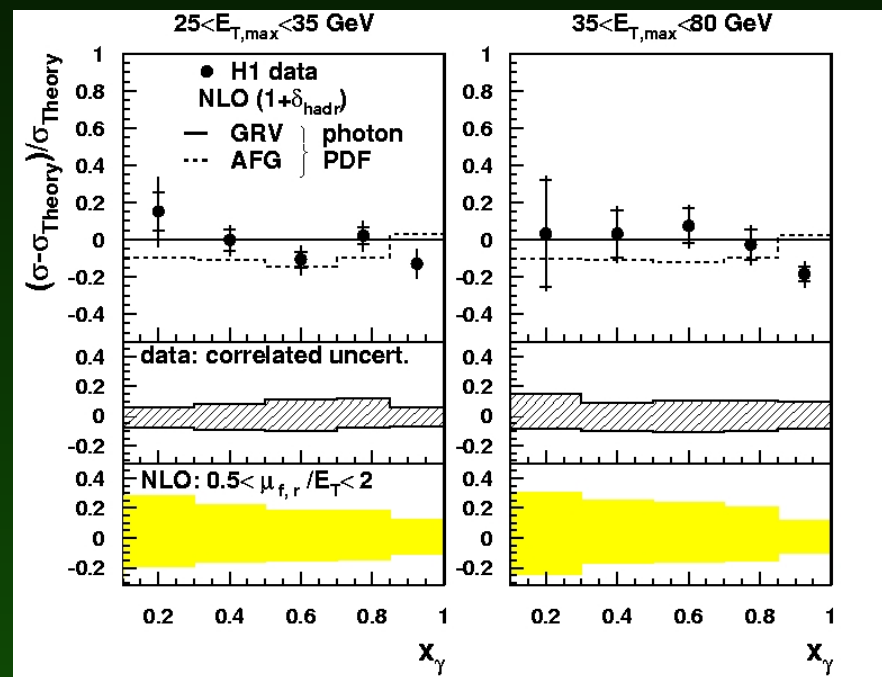
➤ Relative difference between measured and theoretical cross sections

Compare different error contributions to the cross section measurement

Hadronic energy scale:
the MC's describe the
data within $\pm 2\%$.

 energy scale uncertainties

 renormalization and factorization
scale uncertainties NLO calc.



New Energy Weighting Scheme (1)

➤ Weighting procedure

Non iterative procedure using tabulated correction factors ω

on the cell level:

$$E_w = \omega(E_i^0 / Vol_i, E_{group}) \cdot E_i^0$$

- ❖ Evaluate for each cell the energy density (E_i^0 / Vol_i)
- ❖ Determine the energy scale E_{group} for the weighting procedure by searching for groups of neighbour clusters within an η, ϕ – grid
- ❖ Apply the correction factor to each cell of the group E_{group} depending on the energy density

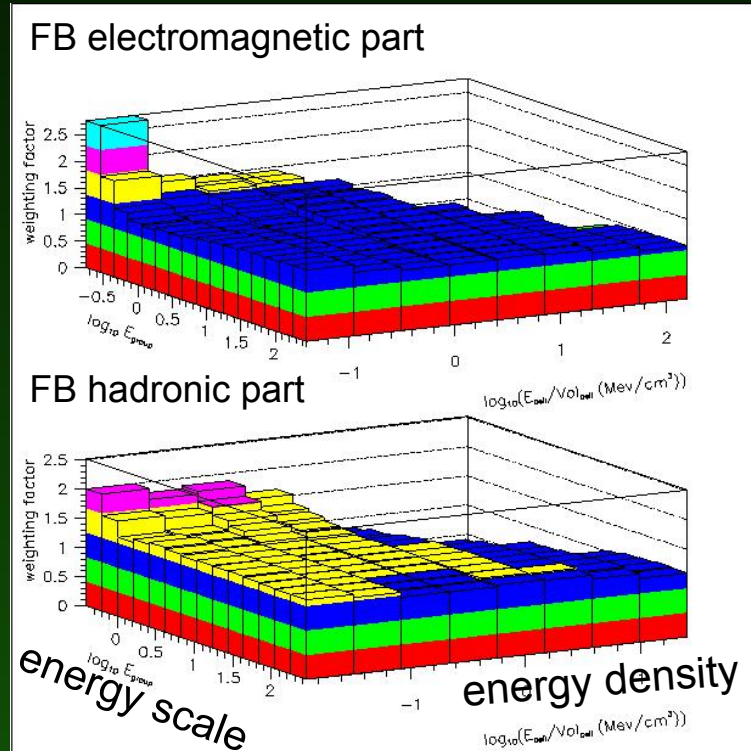
➤ Determination of the weighting factor tables

- ❖ Use single π events simulated in H1 with detailed simulation (low cuts, energy range [50MeV,300GeV], angular range of the LAr calorimeter)
- ❖ The scale of the weighting is determined by the leading energy group E_{group}
- ❖ The true energy E_{True}^i and the measured energy E_i^0 enter 2 D histogramms in the energy density ($\log_{10}(E_i^0 / Vol_i)$) and the group energy ($\log_{10}(E_{group})$)

New Energy Weighting Scheme (2)

➤ Weighting factors

Wheel wise weighting factor tables for the electromagnetic and hadronic part of the LAr calorimeter



➤ Noise correction

Noise cuts on read out level → missing reconstructed energy (few % level at high energies and up 20% at low energies)

➤ Dead material correction

As already discussed

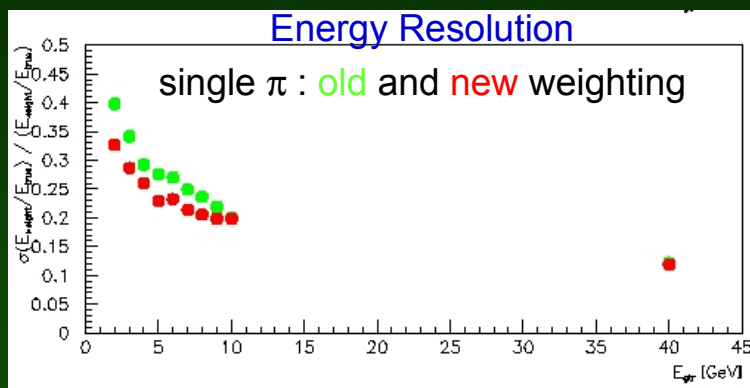
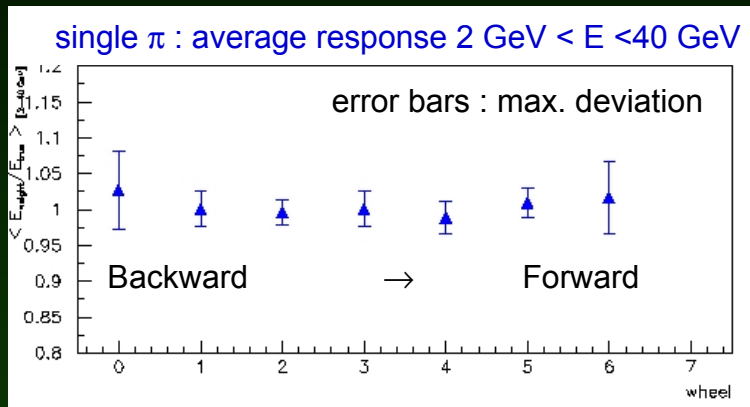
➤ Final calibration using NC DIS data

Determine wheel wise factors by adjusting the average $\langle p_{had}^t / p_e^t \rangle$ for both data and MC to 1

New Energy Weighting Results (1)

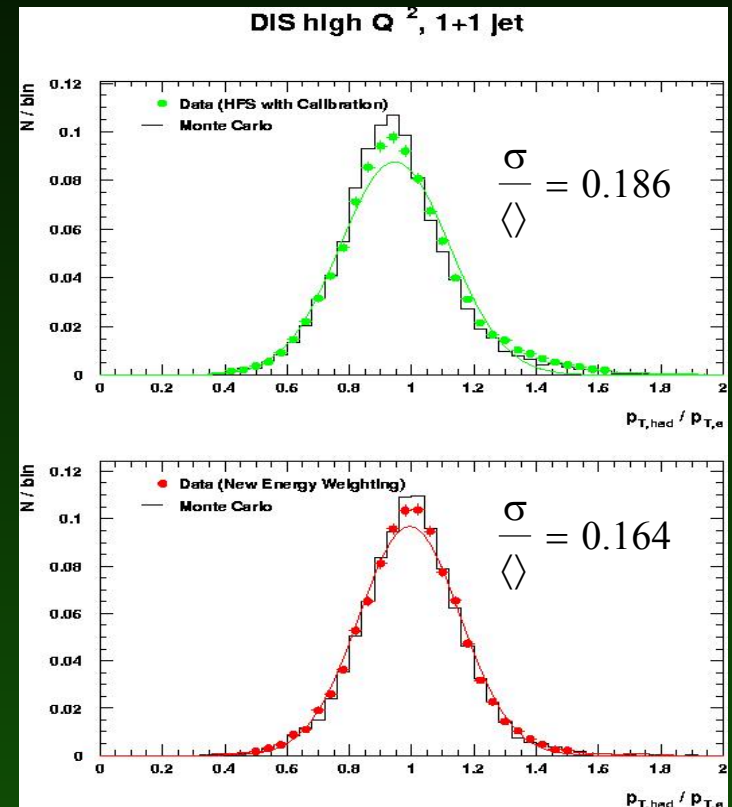
➤ Single π simulation

- ❖ Improved linearity at low E
- ❖ Improved resolution



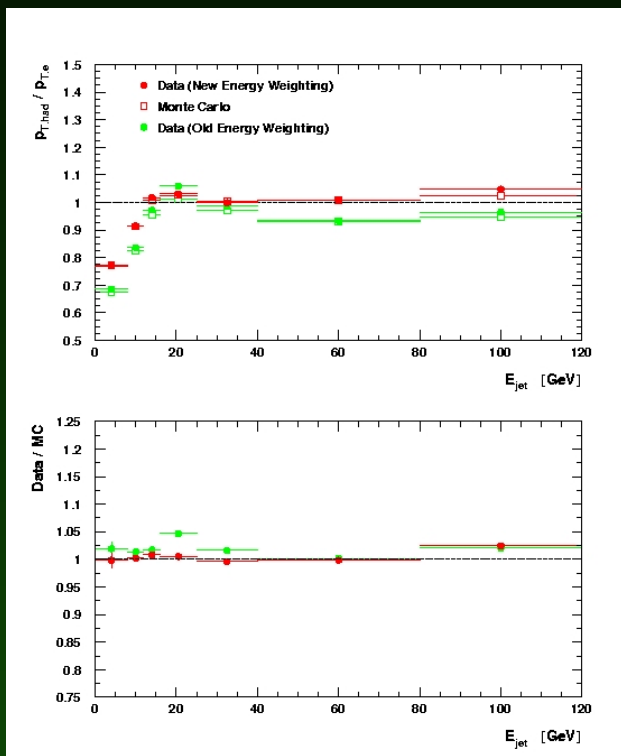
➤ NC DIS high Q^2 data

- ❖ Improved resolution and gaussian shape in p_t balance

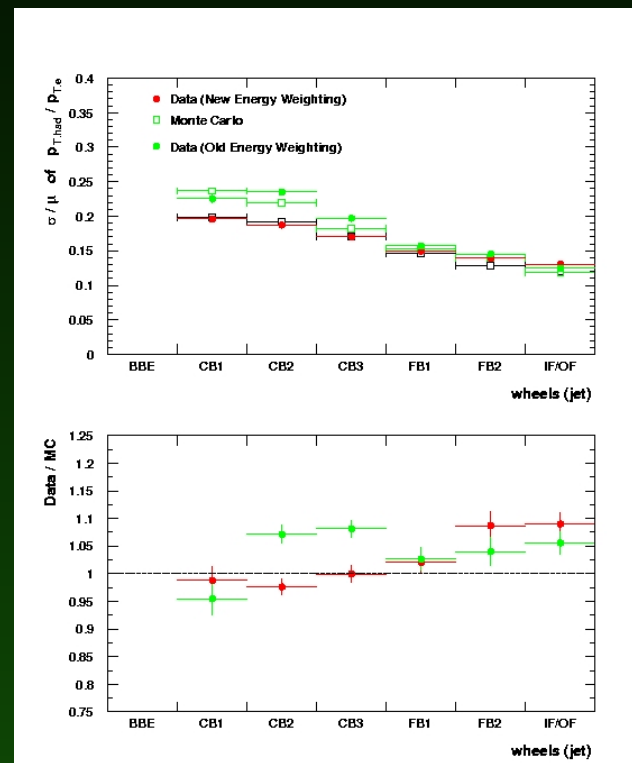


New Energy Weighting Results (2)

- ❖ Jet energy dependence of p_{had}^t / p_e^t
Response improved at low energies



- ❖ Wheelwise resolution in p_{had}^t / p_e^t
Improved resolution at low E



➤ Cluster track combination
needed

- ❖ No p^t dependence $(p_{\text{had}}^t / p_e^t)_{\text{MC/data}}$

Summary

It was a long way to go for H1 from the first beam test setup in 1986 to the 1.4 % data / MC description of the hadronic final state in Neutral Current DIS in 2002.

Good Luck to the ATLAS calorimeter group

